

Facile synthesis of highly efficient Nitrogen-doped Graphene Quantum Dots for Photocatalytic degradation of Organic pollutants

Jeevitha N^{1,3*}, Senthil V², Suresh P³, Kavitha J¹ and Chelladurai C¹

¹Department of Physics and Chemistry, Jai Shriram Engineering College, Tirupur – 638660 India

²Department of Physics and Astronomy, National Institute of Technology, Rourkela – 769008 India

³Department of Physics, Coimbatore Institute of Technology, Coimbatore – 641014 India.

ABSTRACT

A simple and low cost synthetic strategy is used to prepare Nitrogen-doped Graphene Quantum Dots (N-GQDs) through the hydrothermal treatment. The peak shift and formation of new peaks at 26.17° and 43.77° confirmed the doping of nitrogen (N) into GQDs by XRD spectrum. The Raman spectrum identifies the decrement in I_D/I_G value could indicate the removal of hydroxyl and epoxy groups by the hydrothermal treatment. TEM image reveals that the highly crystalline nature and SAED pattern yields the ring shaped pattern. The line profile analyses of the diffraction fringes shows good agreement with the SAED pattern. The UV-vis absorption peak at $\lambda = 235$ nm corresponds to the $\pi \rightarrow \pi^*$ transition of the aromatic C-C bonds and the peak at 297 nm is attributed to $n \rightarrow \pi^*$ transition of C=O bonds. PL emission shows the strong electron affinity of N atoms doped in the graphene oxide by blue shift of peak maximum. The presence of N atoms in GQDs induces the separation of electron-hole pair under UV light and completes the degradation of dye in 110 mins. It suggests that such material exhibit good photocatalytic activity towards the redgradation of Rhodamine B.

Keywords: Graphene oxide; hydrothermal synthesis; photocatalysis; UV-vis absorption.

1. Introduction

Graphene, a flat monolayer of sp^2 bonded carbon tightly packed into a two dimensional (2D) honeycomb lattice, have attracted tremendous attention due to its high surface area, stability, mechanical and electronic properties. More recently, a novel type of luminescent carbon nanomaterial that is graphene quantum dots (GQDs) have fascinated much attention [1-2]. Graphene quantum dots are single atom thick graphene sheets with size smaller than 20 nm, which exhibits some excellent characteristics similar to graphene. The functionalization of graphene is the major route to stabilize graphene suspension in complex environment without agglomeration takes place, which plays a very important role to achieve good interfacial bonding between matrixes and graphene sheets. A lot of research have devoted to finding ways for controllable doping of graphene with electrons and holes. It shows the deposition of different absorbates, either atoms or molecules, on the graphene surface can result in both n- and p-type doping. The chemical doping with heteroatoms is an effective route to tune the intrinsic properties of carbon nanomaterials. Especially, N-

atoms is an excellent element for chemical doping attributed to its comparable atomic size and an electron rich atom which leads to increase the free charge carriers in aromatic ring network [3]. Qian Liu and Beidou Guo et al. reports that the biocompatible nitrogen doped graphene quantum dots as efficient two photon fluorescent probe for cellular and deep tissue imaging. The Nitrogen-doped Graphene Quantum Dots (N-GQDs) prepared by a facile solvothermal method using dimethylformamide (DMF) as a solvent and nitrogen source. In addition, the N-GQDs are non-toxic to living cells and exhibits good photo stability under repeated laser irradiation [4]. Hari Krishna sadhanala et al. reports the synthesis of boron and nitrogen co-doped carbon nanoparticles by a hydrothermal method using sucrose, boric acid and urea as the precursors, which can be used as photoluminescence probe for selective and sensitive detection of picric acid. The sensitivity towards picric acid sensing is high at pH-7 and increases with temperature [5].

Among the reported strategies, the carbon atoms in the aromatic ring replaced by the nitrogen atom induced extensive potential applications like photocatalytic, bio imaging, solar cell, and sensing. In this present study, we have synthesized N-GQDs through the hydrothermal treatment in the presence of graphene oxide (GO) and dimethyl formamide (DMF), without an extra introduction of reducing agents and surface modifier. The prepared samples have been characterized with various analytical techniques such as X-ray diffraction, Ultraviolet visible spectroscopy, Photoluminescence spectroscopy, Transmission electron microscopy and Raman spectroscopy. The N-GQDs exhibit the enhanced photocatalytic activity towards the reduction of organic pollutant Rhodamine B (RhB).

2. Materials and Methods

2.1 Preparation of Graphene Oxide (GO)

GO is prepared by the oxidation of natural graphite powder using the Modified Hummer's method [6]. In typical synthesis, 2 g of natural graphite powder is added to the 1:3 mixture of concentrated $H_2SO_4/KMnO_4$. The reaction mixture is heated to $50^\circ C$ for 2 hours under the continuous stirring for gas release and the double distilled water (DDW) is added slowly. In order to increase the oxidation degree of GO product, the reaction mixture is kept under stirring for next 12 hours. Afterwards, the resultant suspension is terminated by the addition of more DDW followed by a hydrogen peroxide solution (H_2O_2). The solid product is separated and washed with DDW until pH=7. Finally, the obtained solid material is centrifuged and filtered through the membrane filter and vacuum-dried overnight at room temperature.

2.2 Nitrogen Doped Graphene Quantum Dots(N-GQDs)

N-GQDs are synthesized by using 20 ml of DMF added to 0.002g of GO. In which the N atoms from DMF can replace the carbon atoms within the graphene sheet at high temperature. The above mixture is ultrasonicated for 6 hours until the GO colloidal is fully dispersed. Then the final mixed solution is transferred into Teflon lined sealed autoclave maintained at $150^\circ C$ for about 24 hours and then the mixture is cooled down to room temperature. Finally the solid product is washed and dried at $60^\circ C$ for one hour to get the complete precipitation for further study.

2.3 Photocatalytic Activity Studies

Photocatalytic activities of the samples are evaluated by the photocatalytic decomposition of Rhodamine B (RhB). Typically the photocatalyst (0.005 g) is suspended in a 50 ml aqueous solution of RhB ($C_0 = 0.001$ g

in 100 ml). Before turning on the light source, the reaction mixture is sonicated in the dark for 2 hours to reach the absorption-desorption equilibrium between the catalyst and dye molecules. The sonication is confirmed after light irradiation, in order to keep the catalyst suspension throughout the measurements. At given time intervals of illumination, ~5 ml of the mixture is taken, and the UV-spectrum of driven sample is recorded to monitor the degradation behavior. The concentration of clean transparent solution is determined by measuring the absorbance of RhB at 554 nm using a spectrophotometer (UV-2450 Shimadzu UV-visible spectrophotometer). The percentage of degradation is reported as C/C_0 , where C is the absorption of the dye solutions taken at each intervals at maximum absorption peak, and C_0 is the absorption of the initial concentration when the adsorption-desorption equilibrium is reached.

3. Results and Discussion

3.1 XRD study

The X-ray Diffraction pattern (XRD) of GO shows the sharp peak at $2\theta=10.81^\circ$ corresponds to the lattice distance (d_{spacing}) of 0.8174 nm. It is larger than the pristine graphene, due to the lattice expansion of graphene by the oxygen functional groups which clearly indicates that the polar functional groups like hydroxyl and carboxylic groups are presented on the GO surface. The low intensity peak is appeared at $2\theta=26.51^\circ$ corresponds to the (002) plane of graphitic structure of GO with the lattice distance (d_{spacing}) of 0.335 nm, means the presence of few layers of graphene. The sharp and high intensity peak is demonstrated that the well-ordered and layered structure of GO. After the hydrothermal treatment of GO with DMF, the XRD peak position of GO is disappeared in the case of N-GQD-12 hour, but two new broad diffraction peaks are centered at $2\theta=26.17^\circ$ and 43.77° with the typical planes (002) and (111) ascribed to hexagonal structure. Hence, the result illustrates that the lattice distance ($d_{\text{spacing}} = 0.3402$ nm) of nitrogen doped graphene quantum dot is decreased after the hydrothermal treatment of GO [7,8]. That means a significant removal of oxygen functional groups like hydroxyl and carboxylic groups are feasible during the process and a better reducibility due to the successfully synthesized N-doped graphene quantum dot. In addition, the peak of N-GQD at $2\theta=26.17^\circ$ with broader width and weaker intensity than pristine GO is due to the defects produced by the insertion of nitrogen atoms, which means that the degree of disorder increased in the graphene sheet. Various parameters are calculated by the Scherrer equation and listed out in Table (1).

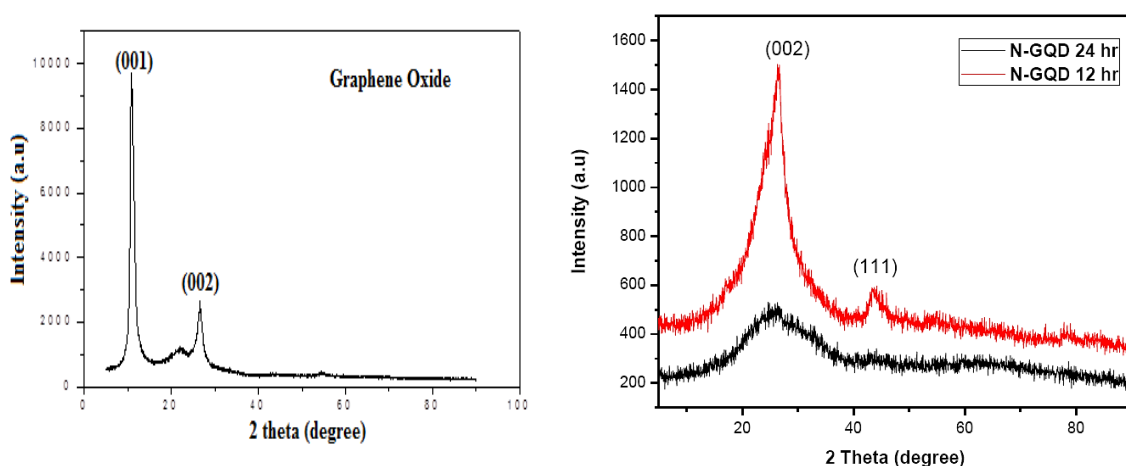


Figure. 1 XRD pattern of GO and N-GQDs prepared by the modified Hummer's method.

Table. 1 Different parameters calculated from XRD pattern

Prepared samples	2θ (degree)	hkl	FWHM (β) (10^{-9}m)	Grain size (D) (10^{-9}m)	d - spacing (d) (10^{-9}m)
N-GQD 12hr	26.17	002	0.1744	0.8068	0.3402
	44.20	111	0.1308	1.1312	0.2046
N-GQD 24hr	26.27	002	0.0708	1.9911	0.3389
	43.77	111	0.0490	3.0176	0.2066

3.2 Raman Study

Raman spectroscopic studies are a suitable technique to characterize the disorder, defect structures, defect density properties of graphene. Figure.2 shows the Nitrogen doped Graphene Quantum Dot (N-GQD 12 hr) exhibit a broader D band at 1328 cm^{-1} and G band at 1570 cm^{-1} . The 2D band occurs at 2635 cm^{-1} suggest that the intercalation of N atoms into the conjugated carbon backbone has led to disordered structure. The intensity of G band is much higher than the D band reveals that the confirmation of Graphene quantum dots. The corresponding I_D/I_G values of N-GQD is seemed as ~ 0.971 , which is less than that of undoped Graphene (~ 1.05)[9]. The decrease in I_D/I_G value could indicate the removal of hydroxyl and carboxyl groups by the hydrothermal treatment. Similarly, the crystalline size has been calculated using the Tuinstra-Koenig (TK) relationship shown in Table. 2. While comparing the spectrum of Figure.2, the sharp intense peak is appeared in 24 hour treated sample due to the strong incorporation of nitrogen atoms in carbon network, causes for the growing of N-GQDs. The high intense 2D peak in 24 hours treated sample indicates the formation of few layers of graphene.

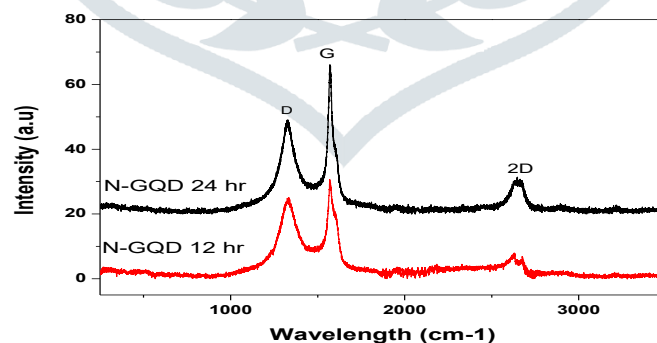


Figure. 2 Raman Spectra of Nitrogen doped graphene quantum dots with 12 hrs and 24 hrs respectively.

Table. 2 Different parameters calculated from the Raman spectrum

Materials	D-band (cm^{-1})	G-band (cm^{-1})	2D band (cm^{-1})	I_D/I_G	I_{2D}/I_G	$L_a(\text{nm})$
N-GQD - 12hrs	1328	1570	2635	0.971	0.883	17.25
N-GQD - 24hrs	1329	1569	2654	0.627	0.247	26.71

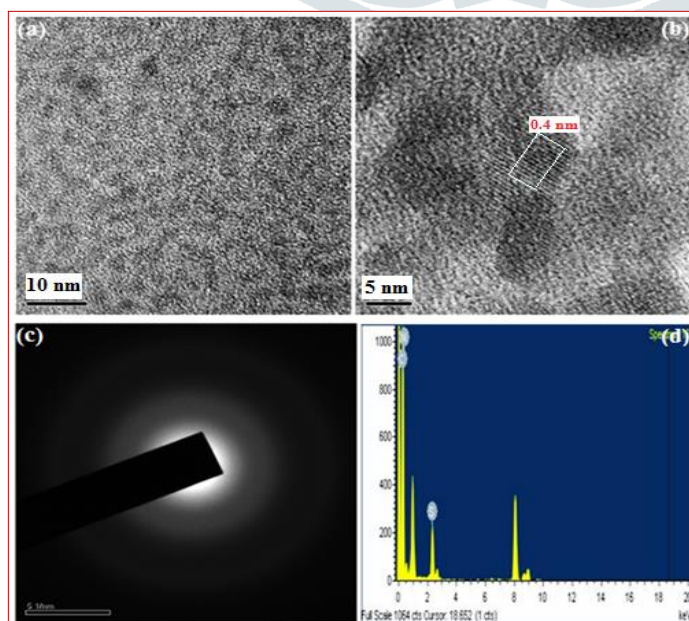
3.3 TEM Image

The TEM analysis is performed to assess the size, uniformity, morphology and microstructure of the composite mainly in graphene. Figure. 3a shows the bright field TEM image of the prepared Nitrogen doped graphene quantum dot. It displays the relatively uniform size distribution without agglomeration of N-GQDs for about 2 nm. HRTEM image of N-GQDs sample(Figure. 3b) reveals that the highly crystalline nature of prepared sample. The morphology is observed to be as identical spherical shapes.

Figure. 3c shows the Selected Area Electron Diffraction (SAED) pattern of N-GQDs, which yields the ring shaped pattern consisting of many diffraction spots for each order of diffraction. The distance between the lattice fringes are about ~ 0.4 nm corresponding to the (002) plane of graphite. The resultant value is slightly larger than that of graphite, which probably caused by the introduction of nitrogen into the hexagonal carbon matrix as well as the presence of unremoved functional groups at the edges of N-GQDs.

Elemental composition of the prepared samples is estimated by EDX analysis and shown in Figure. 3d. The spectrum of N-GQD confirms the presence of Carbon and Nitrogen as main and equal components with low content of sulfur due to the atmospheric stage. Figure. 3e

displays the line profile analysis of the diffraction fringes, which is in good agreement with the SAED pattern.



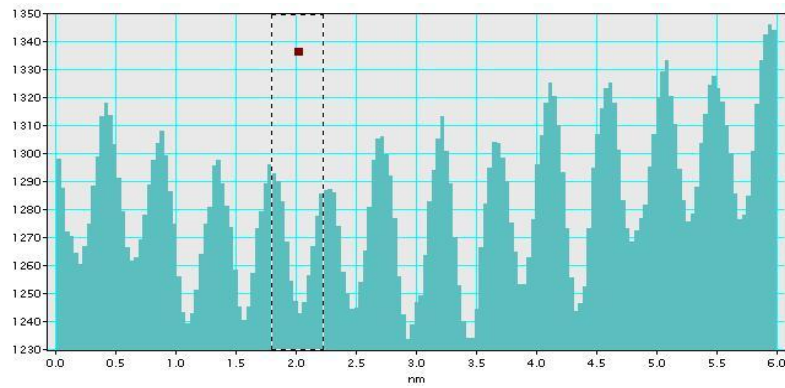


Figure. 3 (a) TEM image of N-GQDs at 24 hrs, (b) HR-TEM image of N-GQDs at 24 hrs, (c) SAED pattern of N-GQDs at 24 hrs, (d) EDX spectrum of N-GQDs sample and (e) the line profile analysis of N-GQDs.

3.4 UV-VIS Absorption Study

Extensive UV-Vis absorption spectroscopy is carried out to understand the optical properties and electronic interaction of graphene materials. The UV-Vis absorption spectrum of GO is shown in Figure. 4. The spectrum of GO exposes two characteristic peaks. The first peak at $\lambda = 235$ nm corresponds to the $\pi \rightarrow \pi^*$ transition of the aromatic C-C bonds. The second peak (shoulder) at 297 nm, can be attributed to $n \rightarrow \pi^*$ transition of C=O bonds. The UV-Vis absorption spectra of N-GQDs in various reaction hours as 12 hours, 24 hours and 48 hours shows a strong absorption peak at 226 nm, 228 nm and 230 nm respectively.

The resultant absorption peak is clearly mentioned that the blue shift by ~ 7 nm with respect to that of graphene oxide. Thus, the result reveals that the doping by N-atoms affected the absorption properties of Nitrogen doped graphene quantum dots due to the decreasing of smaller in size.

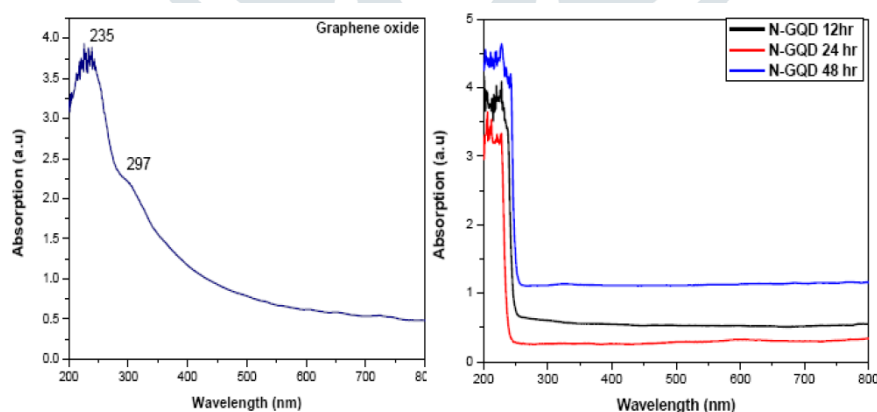


Figure.4 UV-Vis absorption spectra of GO and N-GQDs.

3.5 Photoluminescence Spectra

In the case of optimized N-GQDs exhibit a strong PL emission at 464 nm with the excitation at 320 nm. The 6 nm blue shifts of the PL emission is occurred with respect to GO. Thus, the shift is possible from the strong electron affinity of N atoms doped in the graphene oxide. Moreover, the PL intensity of N-GQDs is

considerably greater than that of GO. The above resultant values predicted that the well ordered formation of N-GQDs. Here, the observed blue shift is occurred at increasing hours due to the high attachment of nitrogen atoms to the aromatic rings which makes the material as small increase in size.

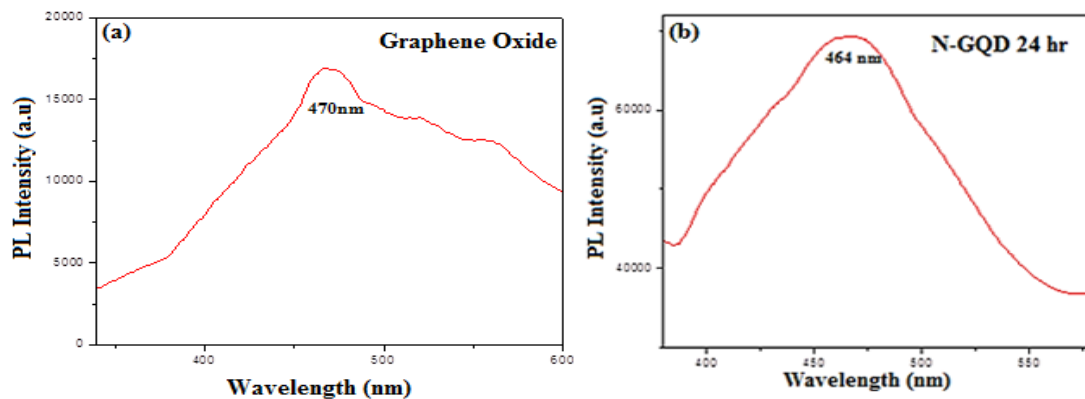


Figure.5 Photoluminescence (PL) spectra of (a) GO and (b) N-GQDs under the excitation

3.6 Photocatalytic Studies

Photocatalytic oxidation is an effective and expensive tool for the removal of organic and inorganic pollutants from water. When the light of appropriate energy illuminates the semiconductor, an electron (e^-) from the valence band is promoted to the conduction band, leaving an electron deficiency or hole (h^+) in the valence band and increases the negative charge in the conduction band (e^-). The electron and hole may migrate to the catalyst surface where they participate in redox reactions with absorbed species [10-15]. The positive hole oxidizes either the pollutant directly or reacts with water to produce hydroxyl radical OH, these hydroxyl radicals (OH) and superoxide radical anions are the primary oxidizing species in the photocatalytic oxidation processes would result in the degradation of pollutants [16-20]. The photocatalytic degradation result of RhB is shown in Figure.6. The initial concentration of RhB decreases with increasing irradiation time. The UV light induced degradation of RhB by N-GQD is most effective. The complete degradation occurred at 110 mins. The efficiency of degradation rate is possible due to the presence of nitrogen doping on graphene which induces the separation of electron-hole pair. The colored solution is transferred into transparent solution shows the complete degradation as shown in Figure.6 photograph.

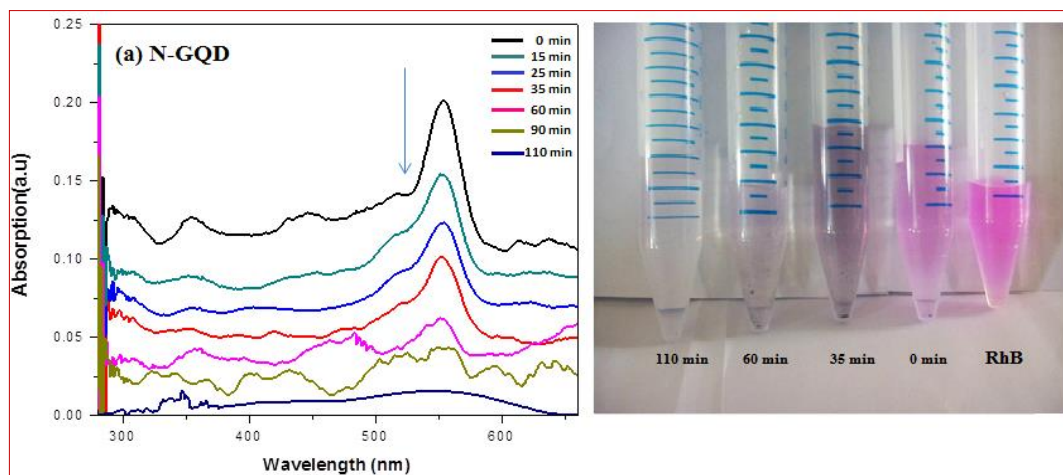


Figure. 6 (a) UV-vis diffuse reflectance spectra of RhB during degradation using N-GQDs

4. Conclusion

In conclusion, N-GQDs are easily prepared by a hydrothermal approach using DMF as solvent and nitrogen source. The results indicated that the nitrogen atoms are successfully incorporated into sp^2 hybridized carbon framework of graphene. The prepared materials are characterized by using XRD, RAMAN, TEM, UV-vis and PL spectroscopy. XRD spectrum confirmed the doping effects by means of observing a shift in the main peak and appearance of new peaks. The Raman analysis for the prepared sample has been proved the defects produced in the graphene sheets and few numbers of layers in the graphene. TEM images confirmed the monodispersion form of quantum dots with the grain size of ~ 2 nm. The optical properties of synthesized samples are analyzed by UV and PL spectrum which reveals that the induced band gap in graphene due to the doping effect. N-GQDs act as a visible light photocatalyst for efficient degradation of Rhodamine B (RhB) under visible light confirms the complete degradation of dye in 110 mins. In future, envision of these kind of materials with enhance in activity will hold great promising in different potential applications.

References

- [1] Cheng, Humin, Jiming Ma, Zhenguo Zhao, and Limin Qi. "Hydrothermal preparation of uniform nanosize rutile and anatase particles." *Chemistry of Materials* 7, no. 4 (1995): 663-671.
- [2] Yoffe, A. D. "Semiconductor quantum dots and related systems: electronic, optical, luminescence and related properties of low dimensional systems." *Advances in physics* 50, no. 1 (2001): 1-208..
- [3] Wang, Xuewan, Gengzhi Sun, Parimal Routh, Dong-Hwan Kim, Wei Huang, and Peng Chen. "Heteroatom-doped graphene materials: syntheses, properties and applications." *Chemical Society Reviews* 43, no. 20 (2014): 7067-7098.
- [4] Liu, Qian, Beidou Guo, Ziyu Rao, Baohong Zhang, and Jian Ru Gong. "Strong two-photon-induced fluorescence from photostable, biocompatible nitrogen-doped graphene quantum dots for cellular and deep-tissue imaging." *Nano letters* 13, no. 6 (2013): 2436-2441.
- [5] Sadhanala, Hari Krishna, and Karuna Kar Nanda. "Boron and nitrogen co-doped carbon nanoparticles as photoluminescent probes for selective and sensitive detection of picric acid." *The Journal of Physical Chemistry C* 119, no. 23 (2015): 13138-13143.
- [6] Hummers Jr, William S., and Richard E. Offeman. "Preparation of graphitic oxide." *Journal of the American Chemical Society* 80, no. 6 (1958): 1339-1339.
- [7] Luo, Zhimin, Dongliang Yang, Guangqin Qi, Jingzhi Shang, Huanping Yang, Yanlong Wang, Lihui Yuwen, Ting Yu, Wei Huang, and Lianhui Wang. "Microwave-assisted solvothermal preparation of nitrogen and sulfur co-doped reduced graphene oxide and graphene quantum dots hybrids for highly efficient oxygen reduction." *Journal of Materials Chemistry A* 2, no. 48 (2014): 20605-20611.

- [8] Choi, Chang Hyuck, Min Wook Chung, Han Chang Kwon, Sung Hyeon Park, and Seong Ihl Woo. "B, N-and P, N-doped graphene as highly active catalysts for oxygen reduction reactions in acidic media." *Journal of Materials Chemistry A* 1, no. 11 (2013): 3694-3699.
- [9] Thu, Tran Viet, Pil Ju Ko, Nguyen Huu Huy Phuc, and Adarsh Sandhu. "Room-temperature synthesis and enhanced catalytic performance of silver-reduced graphene oxide nanohybrids." *Journal of nanoparticle research* 15, no. 10 (2013): 1975.
- [10] Zhang, Yong-Hui, Kai-Ge Zhou, Ke-Feng Xie, Jing Zeng, Hao-Li Zhang, and Yong Peng. "Tuning the electronic structure and transport properties of graphene by noncovalent functionalization: effects of organic donor, acceptor and metal atoms." *Nanotechnology* 21, no. 6 (2010): 065201.
- [11] Jeyalakshmi, V., R. Mahalakshmy, K. R. Krishnamurthy, and B. Viswanathan. "Titania based catalysts for photoreduction of carbon dioxide: Role of modifiers." (2012)..
- [12] Gaya, Umar Ibrahim, and Abdul Halim Abdullah. "Heterogeneous photocatalytic degradation of organic contaminants over titanium dioxide: a review of fundamentals, progress and problems." *Journal of Photochemistry and Photobiology C: Photochemistry Reviews* 9, no. 1 (2008): 1-12..
- [13] Zhu, Peining, A. Sreekumaran Nair, Peng Shengjie, Yang Shengyuan, and Seeram Ramakrishna. "Facile fabrication of TiO₂-graphene composite with enhanced photovoltaic and photocatalytic properties by electrospinning." *ACS applied materials & interfaces* 4, no. 2 (2012): 581-585.
- [14] Xiong, Zhigang, Li Li Zhang, Jizhen Ma, and X. S. Zhao. "Photocatalytic degradation of dyes over graphene-gold nanocomposites under visible light irradiation." *Chemical Communications* 46, no. 33 (2010): 6099-6101.
- [15] Zhuo, Shujuan, Mingwang Shao, and Shuit-Tong Lee. "Upconversion and downconversion fluorescent graphene quantum dots: ultrasonic preparation and photocatalysis." *ACS nano* 6, no. 2 (2012): 1059-1064.
- [16] Mahmoodi, Niyaz Mohammad, Jafar Abdi, Mina Oveisi, Mokhtar Alinia Asli, and Manouchehr Vossoughi. "Metal-organic framework (MIL-100 (Fe)): Synthesis, detailed photocatalytic dye degradation ability in colored textile wastewater and recycling." *Materials Research Bulletin* 100 (2018): 357-366.
- [17] Lin, Yifan, Hao Wan, Fashen Chen, Xiaohe Liu, Renzhi Ma, and Takayoshi Sasaki. "Two-dimensional porous cuprous oxide nanoplatelets derived from metal-organic frameworks (MOFs) for efficient photocatalytic dye degradation under visible light." *Dalton Transactions* (2018).
- [18] Khan, Abdul Qayyum, Shuai Yuan, Sheng Niu, Fengjiang Liu, Guang Feng, Mengci Jiang, and Heping Zeng. "Photocatalytic dye degradation with copper-titanium dioxide nanocomposites under sunlight and visible light irradiation." *Materials Research Express* 5, no. 1 (2018): 015030.
- [19] Liu, Dongliang, Peng Huang, Yong Liu, Zhou Wu, Dongsheng Li, Jun Guo, and Tao Wu. "Cd/In-Codoped TiO₂ nanochips for high-efficiency photocatalytic dye degradation." *Dalton Transactions* 47, no. 17 (2018): 6177-6183.

Figure captions:

Figure. 1 XRD pattern of GO and N-GQDs prepared by the modified Hummer's method.

Figure. 2 Raman Spectra of Nitrogen doped graphene quantum dots with 12 hrs and 24 hrs respectively.

Figure. 3 (a) TEM image of N-GQDs at 24 hrs, (b) HR-TEM image of N-GQDs at 24 hrs, (c) SAED pattern of N-GQDs at 24 hrs, (d) EDX spectrum of N-GQDs sample and (e) the line profile analysis of N-GQDs.

Figure. 4 UV-Vis absorption spectra of GO and N-GQDs.

Figure. 5 Photoluminescence (PL) spectra of (a) GO and (b) N-GQDs under the excitation wavelength of 320 nm.

Figure. 6 (a) UV-vis diffuse reflectance spectra of RhB during degradation using N-GQDs

Table captions:

Table. 1 Different parameters calculated from XRD pattern

Table. 2 Different parameters calculated from the Raman spectrum

